Asynchronous nitrogen supply and demand produce nonlinear plant allocation responses to warming and elevated CO$_2$

Genevieve L. Noyce[a,1], Matthew L. Kirwan[b], Roy L. Rich[a], and J. Patrick Megonigal[a,1]

[a]Smithsonian Environmental Research Center, Edgewater, MD 21037; and [b]Virginia Institute of Marine Science, College of William and Mary, Gloucester Point, VA 23062

Terrestrial ecosystem responses to climate change are mediated by complex plant–soil feedbacks that are poorly understood, but often driven by the balance of nutrient supply and demand. We actively increased aboveground plant-surface temperature, belowground soil temperature, and atmospheric CO$_2$ in a brackish marsh and found nonlinear and nonadditive feedbacks in plant responses. Changes in root-to-shoot allocation by sedges were nonlinear, with peak belowground allocation occurring at +1.7 °C in both years. Above 1.7 °C, allocation to root versus shoot production decreased with increasing warming such that there were no differences in root biomass between ambient and +5.1 °C plots in either year. Elevated CO$_2$ altered this response when crossed with +5.1 °C, increasing root-to-shoot allocation due to increased plant nitrogen demand and, consequently, root production. We suggest these nonlinear responses to warming are caused by asynchrony between the thresholds that trigger increased plant nitrogen (N) demand versus increased N mineralization rates. The resulting shifts in biomass allocation between roots and shoots have important consequences for forecasting terrestrial ecosystem responses to climate change and understanding global trends.

climate change | warming | nitrogen cycling | plants | coastal wetland

Field experiments designed to forecast ecosystem responses to global change often manipulate global change drivers in isolation and neglect interactions that may elicit dramatically different outcomes. Terrestrial ecosystem responses to elevated CO$_2$ (eCO$_2$) are well-characterized (1), but few studies have addressed the combined effects of eCO$_2$ and increased temperature, particularly for intact ecosystems with deep soils (2). Warming and eCO$_2$ often cause opposing effects on net primary productivity (NPP) (3–5), nutrient cycling (6–8), and soil moisture (9), suggesting that responses offset one another with the possibility of no net effect when the 2 factors are combined (4). However, aboveground warming and eCO$_2$ may also have additive effects on NPP (10) and nitrogen (N) pools (11). Overall, the consequences of these coupled global change factors make forecasts difficult because we lack a full mechanistic understanding of feedbacks operating in the system.

Feedbacks between NPP and N cycling are particularly strong in terrestrial ecosystems where N is the primary nutrient limiting plant growth responses to eCO$_2$ in C$_3$-dominated communities (12–14). A global decline in N availability to plants suggests that progressive N limitation is developing as plants respond to factors such as eCO$_2$ and longer growing seasons (15). Changes in the balance of plant N demand and N availability are one source of the complexity observed in terrestrial ecosystem responses to global change as plants optimize resource acquisition by shifting NPP allocation between roots and shoots. Allocation to roots governs soil C stocks, C turnover time (16–19), microbially mediated biogeochemical cycles (20), and physical processes such as erosion (21). The capacity of plants to dynamically allocate growth aboveground or belowground to optimally forage for resources is fundamental to terrestrial ecosystem responses to climate change

and can be understood only in an experimental context through manipulations that incorporate both aboveground and belowground components.

Through feedback-controlled heating, we actively manipulated whole-ecosystem temperature (aboveground plant surface and belowground soil) in a tidal marsh where herbaceous plant communities are known to respond rapidly to environmental change (13). The Salt Marsh Accretion Response to Temperature eXperiment (SMARTX) was deployed in 2 sites representing plant communities with distinctly different responses to global change. The "C$_3$ site" is dominated by the C$_3$ sedge *Schoenoplectus americanus* and is relatively wet due to frequent tidal flooding, while the "C$_4$ site" is dominated by the C$_4$ grasses *Spartina patens* and *Distichlis spicata* and is relatively dry. Replicate transects at each site have a warming gradient ranging from an unheated ambient plot to plots that are heated year-round to 1.7, 3.4, and 5.1 °C above ambient (*SI Appendix*, Figs. S1–S3). Four levels of whole-system heating allowed us to detect nonlinear response patterns, a distinct advantage for process-oriented experiments over the typical 2-level design. Warming spans from above the plant canopy to 1.5-m soil depth. At the C$_3$ site, there are also eCO$_2$ plots crossed with ambient and +5.1 °C warming treatments (*SI Appendix*, Fig. S1). CO$_2$ treatments were not implemented in the C$_4$ site as extensive prior research at this site indicates that the C$_4$ grasses are minimally responsive to eCO$_2$ (22), although we acknowledge that is not universally the case (23). This design allows us to capture the variable responses to

Significance

Interactions between nutrient supply and plant demand dictate key terrestrial ecosystem feedbacks to global climate change. We investigated these responses in a marsh ecosystem and found that plants and soils respond to warming at different temperatures. Modest warming caused plant demand for nitrogen (N) to outpace the soil N supply, while more extreme warming caused the N supply to outpace plant N demand. These responses changed when elevated CO$_2$ was added to the warming treatments. Globally, terrestrial plant N demand has exceeded soil N supply in unfertilized ecosystems over the past century; our results reveal that this imbalance is driven primarily by elevated CO$_2$ and forecast that N supply will likely increase over plant demand as warming exceeds 2 °C.

differing levels of warming in 2 physiologically distinct plant communities and to assess the interactions between 2 global change factors in 1 community dominated by species with the ubiquitous C_3 photosynthetic pathway. We present data from the first 2 complete growing seasons for which both temperature and CO_2 were manipulated (2017 and 2018). Warming treatments began 10 mo earlier (June 2016), allowing time for possible transient effects from the step increase in temperature to resolve. The 2 growing seasons varied dramatically in precipitation, with 89 cm in 2017 and 171 cm in 2018; the 30-y mean is 106 cm (1981 to 2010, National Oceanic and Atmospheric Administration). See *Materials and Methods* for full experimental details.

Warming Had Differing Effects on C_3 and C_4 Plant NPP

Warming elicited distinctly different plant responses in the C_3-dominated community compared to the C_4-dominated community, as observed in terrestrial grasslands (10). Total NPP at the C_3 site increased by 18 to 22% in the +5.1 °C plots compared to the ambient plots, but the effect was not statistically significant at intermediate warming levels (ANOVA: $F_{3,15} = 1.67$, $P = 0.216$; *SI Appendix*, Tables S1 and S2). In contrast, total NPP at the C_4 site significantly declined with +5.1 °C of warming in 2017 from 484 to 329 g·m^{-2} ($P = 0.038$; *SI Appendix*, Table S5), an effect that was absent under the unusual environmental conditions of 2018 ($P = 0.9$; *SI Appendix*, Table S5) (Fig. 1). The negative effect of warming on C_4 grass NPP in 2017 occurred despite a longer growing season with shoots emerging 2 wk earlier in the +5.1 °C plots compared to the ambient controls. In both years, C_3 shoots emerged 4 wk earlier and senesced up to 4 wk later, which resulted in 13 to 20% of the total aboveground NPP being produced during this first month of green-up in the warmed plots (*SI Appendix*, Fig. S4).

Grasslands, including coastal wetlands, are considered model systems for global change experiments because annual plants

rapidly respond to global change factors (4, 13, 22). However, tidal grasslands (i.e., marshes) may behave differently from terrestrial grasslands where soil moisture commonly limits plant and microbial responses to eCO_2 and warming (10, 24, 25). Prior experiments found both positive and negative NPP responses to warming in marshes (26–31) and other grasslands (4, 10, 24, 25) depending on plant species and climate, although the majority of studies consider only C_4 plants. Studies focused on C_4-dominated tidal marshes have reported that warming consistently increases the aboveground biomass of *Spartina alterniflora* (28), but the responses of the C_4 species *S. patens* and *D. spicata*, which occupy relatively higher elevations, increase in some studies (29–31) and not in others (28). Latitudinal gradients also suggest that *S. alterniflora* aboveground productivity will increase with warming up to a threshold (32), although biomass negatively responds to above-average temperatures (33). One of the few studies to include both C_3 and C_4 plants found that 3 °C of aboveground warming increased aboveground biomass of both groups (27).

Traditionally, warming responses have been interpreted in the context of an optimal temperature for metabolism, where rates of productivity increase up to the point of typical summer temperatures and then decline with increased warming (34, 35). Alternatively, we propose that the negative C_4 response observed in 2017 was due to water stress, as the C_4 grasses have shallower root systems than the C_3 sedge and the C_4 site is located in a higher, drier area of the marsh. Although the C_4 photosynthetic pathway allows CO_2 assimilation to proceed under low stomatal conductance to conserve water (36), the combination of increased evaporative demand of transpiration with warming, relatively low soil moisture at the soil surface, and the shallow rooting depth likely drove the net negative effect. In contrast, the high precipitation in 2018 likely reduced warming-related water stress and led to high total NPP.

Root-to-Shoot Ratio Responds Nonlinearly to Warming

Root-to-shoot ratio is a sensitive index of the balance of plant N demand versus supply in most terrestrial ecosystems. In the C_3 community, warming altered both belowground NPP (ANOVA: $F_{3,15} = 4.64$, $P = 0.017$; *SI Appendix*, Table S1) and the root-to-shoot ratio (ANOVA: $F_{3,15} = 4.52$, $P = 0.019$; *SI Appendix*, Table S1), but these effects were nonlinear (Fig. 2 and *SI Appendix*, Table S2). Belowground NPP in the C_3 community increased in response to modest warming of +1.7 °C from 98 to 208 g·m^{-2} under normal precipitation in 2017 ($P = 0.001$; *SI Appendix*, Table S5) and then declined with further warming back to the NPP of the ambient treatment ($P > 0.5$) (Fig. 2). As a result, modest warming nearly tripled the root-to-shoot ratio from 0.27 to 0.73 ($P = 0.010$; *SI Appendix*, Table S5), whereas higher warming levels of +3.4 and +5.1 °C were not different from ambient ($P > 0.8$) (Fig. 2). Root biomass was lower across all treatments in 2018 (Fig. 2), but again plots warmed by +1.7 °C had twice the root biomass of ambient plots (96 compared to 46 g·m^{-2}), although in this case the means were not significantly different ($P = 0.4$; *SI Appendix*, Table S5). The C_4 community exhibited a similar, but muted, response of fine root NPP and root-to-shoot ratio to whole-ecosystem warming (Fig. 3). In 2017, modest warming of 1.7 °C increased the root-to-shoot ratio from 0.287 at ambient to 0.488 ($P = 0.022$; *SI Appendix*, Table S5), although this pattern did not repeat in the high precipitation year of 2018, and thus the response was not significant across the full 2-y period ($P = 0.7$). Nonlinear responses such as those observed in the C_3 community have not been reported previously because experiments in other ecosystems generally have one treatment level and test a comparatively small range of warming treatments, achieving 1 to 2 °C of soil warming confined to the upper 5 cm (refs. 30 and 37–39, but see ref. 40 for an exception).

Like most terrestrial ecosystems, this site is N-limited (41). Whole-ecosystem warming by 1.7 °C in the C_3 community increased
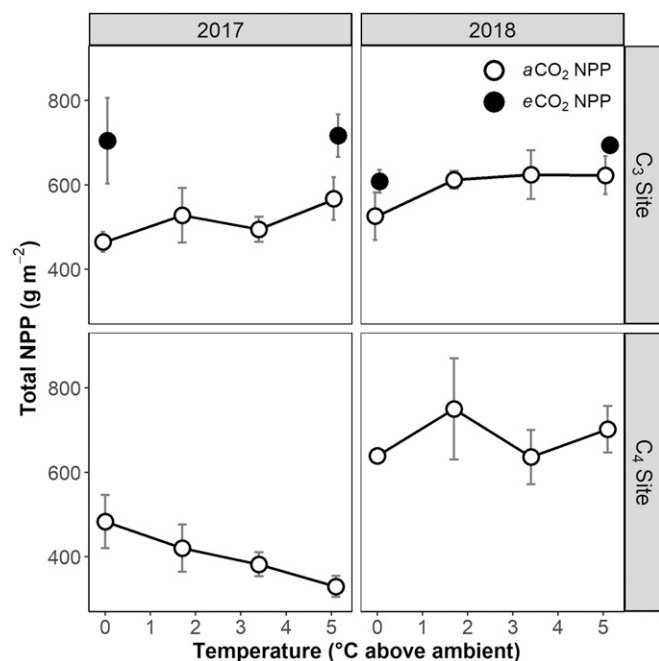

Fig. 1. Changes in total NPP for 2017 and 2018 in response to warming and eCO_2 in both plant communities. Circles represent treatment means ($n = 3$) ±1 SE. Open circles are aCO_2 plots; closed circles are eCO_2 plots. Full model results are provided in *SI Appendix*, Tables S1–S7. Pairwise comparisons between means are provided in *SI Appendix*, Tables S5 and S8.

Noyce et al.

Fig. 2. Changes in shoot and fine-root productivity (*Top*), root-to-shoot ratio (*Middle*), and porewater NH_4 (*Bottom*) in response to warming and eCO_2 in the C_3 community. Circles, triangles, and squares represent treatment means ($n = 3$) ±1 SE. Open circles, triangles, and squares are aCO_2 plots; closed circles, triangles, and squares are eCO_2 plots. Full model results are provided in *SI Appendix*, Tables S1–S7. Pairwise comparisons between means are provided in *SI Appendix*, Tables S5 and S8.
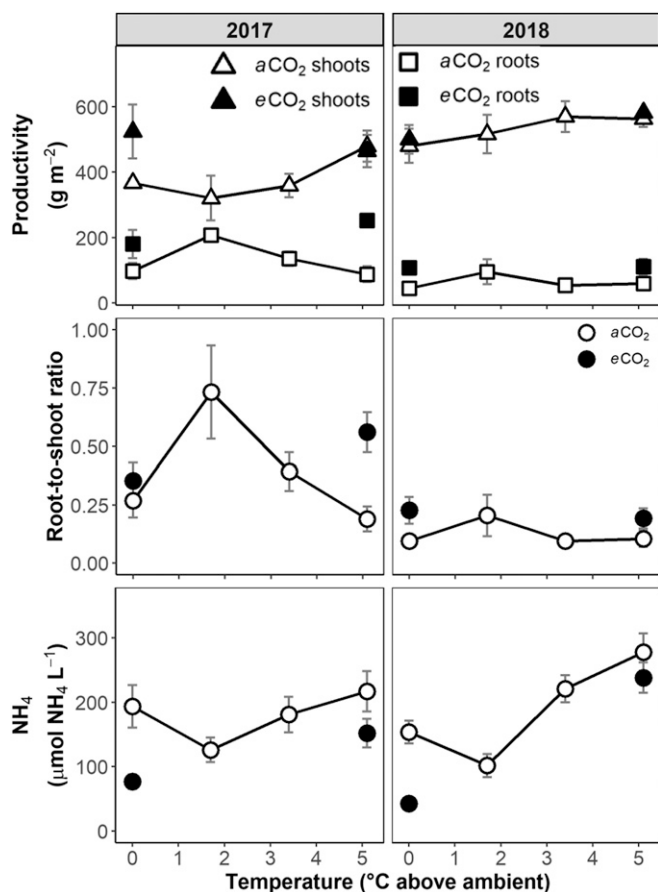
total NPP from 465 to 528 g·m^{-2} in 2017 (Fig. 1 and *SI Appendix*, Table S5) and thus increased plant N demand from 410 to 471 g N·m^{-2} (Fig. 4A and *SI Appendix*, Table S5). Supporting evidence for the increase in plant N demand is the large shift in growth allocation to fine roots, a well-documented response to N-limitation in terrestrial ecosystems (42, 43). This shift in root-to-shoot allocation could occur only if the warming-forced increase in plant N demand (42, 43) was larger than the warming-forced increase in soil N mineralization rate. Stimulation of N mineralization by warming is expected based on previous active and passive warming studies (2, 6, 44–46), but such studies are rarely designed to quantify response surfaces. Porewater NH_4 concentrations varied nonlinearly with warming in the C_3 community (ANOVA: $F_{3,15} = 3.92$, $P = 0.030$; *SI Appendix*, Table S1), declining with +1.7 °C of whole-ecosystem warming (Fig. 2 and *SI Appendix*, Table S2). We propose that soil warming of +1.7 °C was not sufficient to offset the increase in plant N demand because porewater NH_4 concentrations declined compared to ambient conditions (*SI Appendix*, Table S2) from 198 to 126 µmol NH_4 L^{-1} in 2017 ($P = 0.059$; Fig. 2 and *SI Appendix*, Table S5), and from 154 to 102 µmol NH_4 L^{-1} in 2018 ($P = 0.8$; Fig. 2 and *SI Appendix*, Table S5), a response that consistently accompanies increased plant N demand in this NH_4-dominated system (13).

When whole-ecosystem warming in the C_3 plant community exceeded 1.7 °C, porewater NH_4 concentrations began to increase

(Fig. 2 and *SI Appendix*, Tables S2 and S5) despite constant or increasing NPP (Fig. 2 and *SI Appendix*, Tables S2 and S5) and plant N uptake (Fig. 4A and *SI Appendix*, Tables S2 and S5). We saw the same pattern in both 2017 and 2018, demonstrating that this is not a short-term transient effect. In response to higher N availability, plants shifted allocation from belowground structures to aboveground structures (Fig. 2). Plots with higher concentrations of porewater NH_4 had consistently lower root biomass (Pearson's correlation: $r = -0.39$, $P = 0.02$; Fig. 5) across both years, supporting this mechanism. C_4 belowground productivity did not show the same trend. We propose that the same biogeochemical mechanisms operate in both plant communities, but they are less dominant in the C_4 community due to plant physiological traits that are specific to the C_4 species in this system. In particular, the dominant C_4 species (*S. patens*) has a lower affinity for N uptake than the dominant C_3 species (*S. americanus*) (47) and may therefore be relatively insensitive to changes in N availability at in situ rates of mineralization.

Our results suggest that plants and microbes have different sensitivities to whole-ecosystem warming, as illustrated in Fig. 6. Plants respond relatively more strongly than N mineralization to low levels of warming, driving up plant N demand, and thus increase allocation to root biomass in order to acquire enough N to sustain the higher NPP. At a certain threshold (between 1.7 and 3.4 °C of warming in this system), warming increases N mineralization to the point that plants can acquire sufficient N with
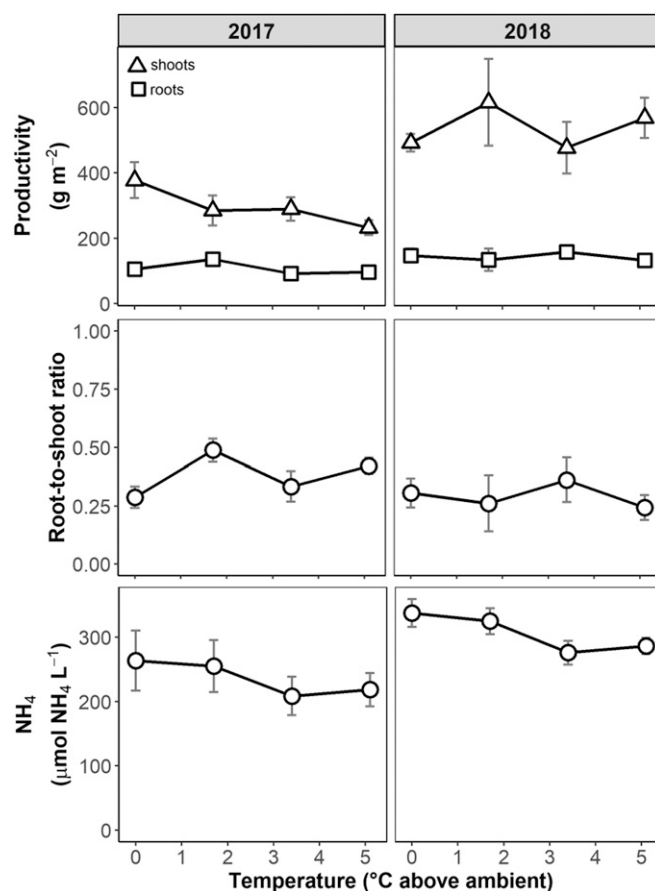
Fig. 3. Changes in shoot and fine-root productivity (*Top*), root-to-shoot ratio (*Middle*), and porewater NH_4 (*Bottom*) in response to warming in the C_4 community. Circles, triangles, and squares represent treatment means ($n = 3$) ±1 SE. Full model results are provided in *SI Appendix*, Tables S1–S7. Pairwise comparisons between means are provided in *SI Appendix*, Tables S5 and S8.
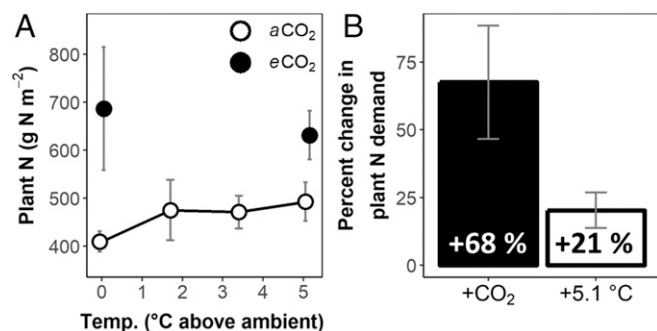
Fig. 4. Changes in plant nitrogen in C_3 community in 2017. (*A*) Total nitrogen stored in roots and shoots under warming and eCO_2. Circles represent treatment means (*n* = 3) ±1 SE. Open circles are aCO_2 plots; closed circles are eCO_2 plots. (*B*) Increase in plant nitrogen demand relative to ambient conditions under elevated CO_2 (black) and 5.1 °C of warming (white). Bars represent treatment means (*n* = 3) ±1 SE. Full model results are provided in *SI Appendix*, Tables S1–S7. Pairwise comparisons between means are provided in *SI Appendix*, Tables S5 and S8.

less investment in root production, allowing more investment in aboveground tissues.

A recent cross-system meta-analysis found that warming generally increased both above- and belowground NPP, but the scale and direction of the response depended on both the heating method and magnitude (2). Warming achieved passively with chambers has negligible effects on soil temperature, and active aboveground-only warming with infrared heaters typically raises soil temperatures by <2 °C and only to shallow depths (37–39). Although in some ecosystems passive chambers are able to raise soil temperature by 1 to 1.5 °C during the summer (30), they do not yield consistent temperature differentials throughout the day, can decrease in effectiveness over time, and are effective only during the growing season (29, 30). A recent wetland experiment reported that passive chambers also decoupled aboveground and belowground responses by warming the air while cooling the soil (48). These experimental designs are unlikely to capture the asynchronous, nonlinear patterns that we observed in SMARTX, which arose from the balance of different warming-response curves for plant versus soil microorganisms.

Elevated CO_2 Increases Belowground Productivity

Single-factor warming studies alone are not sufficient to predict the response of C_3 plants to temperature because they do not address the interactive effects of eCO_2. We found that the perceived ecosystem consequences of warming significantly change when $eCO_2 \times$ warming interactions are considered.

It is well established that eCO_2 increases C_3 NPP at this site (22), but the combined effects of warming and eCO_2 on NPP have not previously been studied. As expected, eCO_2 significantly increased total NPP across both years (ANOVA: $F_{1,20}$ = 13.94, *P* = 0.001; *SI Appendix*, Tables S6 and S7). Elevated CO_2 also significantly increased root NPP (ANOVA: $F_{1,15}$ = 29.65, *P* < 0.001; *SI Appendix*, Tables S6 and S7), leading to significant increases in root-to-shoot ratio (ANOVA: $F_{1,15}$ = 19.50, *P* < 0.001; *SI Appendix*, Tables S6 and S7) (Fig. 2). In 2017, eCO_2 nearly doubled belowground NPP under ambient temperatures (98 versus 181 g·m^{-2}, *P* = 0.047; *SI Appendix*, Table S8) and almost tripled belowground NPP when crossed with +5.1 °C of warming (88 versus 253 g·m^{-2}, *P* < 0.001; *SI Appendix*, Table S8) (Fig. 2). The same pattern occurred in 2018, with belowground NPP increasing from 46 to 109 g·m^{-2} under ambient temperatures (*P* < 0.001; *SI Appendix*, Table S8) and from 60 to 111 g·m^{-2} when crossed with +5.1 °C of warming (*P* = 0.1; *SI Appendix*, Table S8) (Fig. 2). Similar responses have been observed in upland

sites, where root biomass responded more strongly to eCO_2 than to warming (49). As under +1.7 °C of warming, the high plant investment in belowground NPP under eCO_2 likely reflects an increase in N demand and thus more allocation of growth to roots. Although warming by +5.1 °C would also have accelerated rates of N mineralization as in the C_3 warming-only plots, eCO_2 stimulation of total NPP created relatively more plant N demand (ANOVA: $F_{1,8}$ = 8.078, *P* = 0.022; *SI Appendix*, Table S6) (Fig. 4*A*) and significantly lowered porewater NH_4 concentrations (ANOVA: $F_{1,20}$ = 0.031, *P* = 0.031; *SI Appendix*, Table S6) (Fig. 3). There was no difference in shoot NPP between the +5.1 ambient CO_2 (aCO_2) plots and the +5.1 eCO_2 plots in either year (*P* > 0.3; *SI Appendix*, Table S8) (Fig. 2), indicating that the effects of eCO_2 and warming were not additive in this C_3-dominated ecosystem and illustrating the need to consider interacting climate change factors together rather than in isolation.

Implications for Ecosystem Responses to Warming and eCO_2

Globally, terrestrial plant N demand has exceeded soil N supply in unfertilized ecosystems over the past century, which Craine et al. proposed is likely due to either increasing atmospheric CO_2 or a longer growing season (15). In our experimental system, eCO_2 was the dominant driver of this phenomenon in a typical precipitation year, increasing plant N uptake by 68% over ambient conditions (*P* = 0.028; *SI Appendix*, Table S8), while warming of 1.7 and 5.1 °C increased it by 15 and 21% (*P* > 0.5; *SI Appendix*, Table S5), respectively (Fig. 4*B*). Global temperatures have increased about 0.85 °C over the past century (50), which is below the 2 °C threshold where whole-ecosystem warming increased N supply in the present study (Fig. 6). Our results uniquely suggest that soil N supply may begin to meet or exceed plant N demand when warming exceeds 2 °C as forecast (51), thereby potentially mitigating N limitation of plant eCO_2 responses in N-limited ecosystems, particularly those with C-rich soils. It is possible that plant and microbial responses to warming may change over time periods longer than the 3 growing seasons of this experiment (40), necessitating ongoing observations.

Plants universally increase root growth in response to N limitation (42, 43), and allocation of growth to roots regulates important ecosystem processes such as C stabilization (16, 18, 19). In coastal wetlands, allocation to roots regulates soil elevation gain by adding organic material directly to the soil profile, thereby influencing the future stability of wetlands, and thus their C sink, to accelerated sea level rise (52). Rising atmospheric CO_2 has contributed to an increase in land C sinks over recent decades, but the future influence of eCO_2 is expected to be increasingly mediated by direct temperature effects on plant physiology (5, 53) or indirect temperature effects via interactions with factors such as precipitation and N availability (13, 15). Grasslands, including coastal marshes, are considered model systems for forecasting the
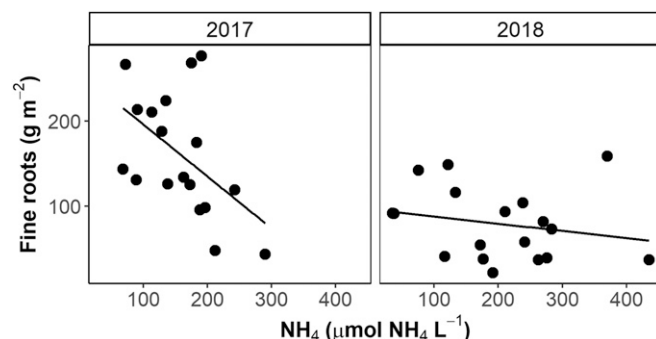

Fig. 5. Porewater NH_4 concentration vs. fine-root biomass for C_3 community in 2017 and 2018.
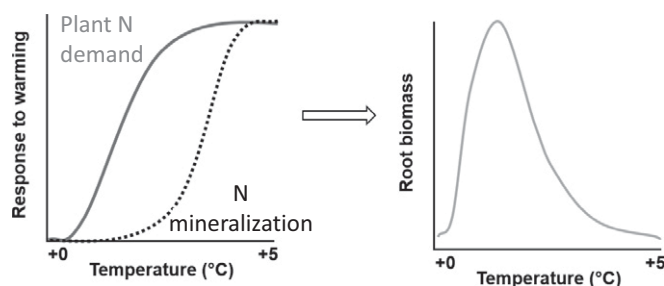
Fig. 6. Conceptual diagram showing how plants are more sensitive to modest warming than the microbial community, creating a disconnect between plant N demand and N mineralization rates that leads to a large increase in root biomass around 2 °C of warming that declines with additional warming.

effects of global change, and our whole-ecosystem responses to warming suggest that the present balance of plant N demand and soil N availability may shift as the planet warms beyond the 2 °C goal of the Paris Agreement.

Materials and Methods

Site Description and Experimental Design. SMARTX was established in the Smithsonian's Global Change Research Wetland (GCReW) in 2016. GCReW is part of Kirkpatrick Marsh, a brackish high marsh on the western shore of the Chesapeake Bay, United States (38°53′ N, 76°33′ W). Soils are typically saturated to within 5 to 15 cm of the soil surface, but flood frequency varies across the site. In the high elevation areas where the C_4 grasses *S. patens* and *D. spicata* dominate, flooding occurs in 10 to 20% of high tides, whereas, in lower areas where the C_3 sedge *S. americanus* dominates, flooding occurs in 30 to 60% of tides.

SMARTX consists of 6 replicate transects, 3 located in each of the 2 dominant plant communities (C_3 sedge community and C_4 grass community). Each transect is an active heating gradient consisting of unheated ambient plots and plots that are heated to 1.7, 3.4, and 5.1 °C above ambient. Transects were designed to have similar plant composition across their length. The intent of the gradient design is to generate response curves that allow us to propose novel mechanisms for ecosystem responses to a warming climate. All plots are 2 × 2 m, surrounded by a 0.2-m buffer to mitigate edge effects. Aboveground plant-surface temperature is elevated with infrared (IR) heaters, and soil temperature is elevated with vertical resistance cables (54). The temperature gradient is maintained by integrated microprocessor-based feedback control to create a fixed temperature differential from the ambient temperature for each plot (54) (*SI Appendix*, Figs. S2 and S3). Soils are heated to 1.5 m depth, which is the depth most vulnerable to climate or human disturbance, and the design maintains the natural downcore pattern of declining soil temperature and temperature variability in increasing depth. Direct soil heating provides better control than heaters alone and counteracts limitations of IR heaters in ecosystems with high soil moisture, dense plant canopy cover, and/or heat loss to the surrounding soil matrix and is the only practical way to penetrate to deeper soil horizons (54). Four to 6 1,000-W heaters (FTW-1000, Mor Electric Heating Assoc. Inc., Comstock Park, MI) are located above each heated plot, and heater wattage output is regulated continuously via pulse-width modulation of power output based on the difference in temperature between the ambient and heated plots. The soil-warming techniques use vertical warming "pins" made from resistance cable that are inserted into a 50-cm grid across the plots. Ambient plots have dummy pins to emulate site disturbance. Aboveground and belowground temperature variation is assessed via thermocouples embedded in acrylic plates at plant canopy level or inserted directly into the soil (54). Warming began on June 1, 2016, and the treatment is applied 365 d per year.

At the C_3 site, there are 6 additional plots with eCO_2 chambers. These consist of 2-m-diameter open-top chambers (41) with a target atmospheric CO_2 concentration of 750 to 800 ppm. CO_2 concentrations are independently controlled at each plot using K30 sensors (CO2Meter Inc., Ormond Beach, FL) with continuous feedback control. Three chambers are at ambient temperatures and 3 are heated to +5.1 °C above ambient, again using IR heaters and vertical resistance cables. CO_2 is manipulated only during daylight hours of the growing season (2017: April 11 to November 30; 2018: April 26 to December 6).

Productivity. Annual belowground productivity in all plots was assessed using root ingrowth cores. To account for variability, 3 mesh bags (5-cm diameter,

25-cm length in 2017 and 40-cm length in 2018) filled with root-free peat were inserted into each plot in November and retrieved 12 mo later. Roots and rhizomes were picked out of each core, separated into functional groups, oven-dried at 60 °C, and then weighed. In the present analysis we used only fine root biomass, which underestimated total belowground productivity but reduced the high variability introduced by the presence or absence of rhizomes, which the ingrowth bag technique does not adequately sample. After drying, replicate cores were combined, ground, packed into tin capsules, and analyzed for C, N, ^{13}C, and ^{15}N on a Thermo Delta V Advantage mass spectrometer coupled to an Elementar vario ISOTOPE Cube Elemental Analyzer at the Smithsonian MCI Stable Isotope Mass Spectrometry Laboratory.

Annual aboveground productivity of *S. americanus* stems was assessed using a combination of nondestructive allometry measurements made at peak biomass (2017: July 31 to August 1; 2018: July 30 to July 31) and tracking of individual stems throughout the growing season (2017: March 20 to October 18; 2018: April 11 to November 14). During peak biomass, we measured the density, height, and width of *S. americanus* stems in 5 to 6 30- × 30-cm subplots in each treatment plot. Allometric equations were used to convert allometry data to standing biomass (55). Individual *S. americanus* stems (2017: n = 439; 2018: n = 532) were tracked and measured weekly (March to May) or biweekly (June to November). Total *S. americanus* productivity per plot was estimated as

$$productivity = biomass + \left[frac_{dead} * biomass \right] + \left[frac_{new} * biomass \right],$$

where $frac_{dead}$ was the fraction of stems that senesced prior to the census (2017: 35%; 2018: 21%) and $frac_{new}$ was the fraction of stems that emerged after the census (2017: 4.8%; 2018: 15%), as these stems were not included in the peak biomass estimates.

Measuring the allometric dimensions of individual grass stems is not logically feasible, so we used destructive sampling for the 2 grass species. Less than 5% of C_4 grasses senesced prior to August 1 in both years, so peak biomass reasonably approximates annual aboveground productivity. Grasses in 5 to 6 25-cm^2 subplots in each plot were clipped at the soil surface, dried, and weighed, and the dry weights were scaled to the plot level. Dried samples of all species were combined by plot, ground, and analyzed for C and N content in the same manner as the roots.

Other (nongrass) species growing in the subplots during the summer census were also measured, and their respective biomass was calculated using allometric equations. (55).

Porewater Sampling and Analysis. Porewater samples were collected in July of each year using stainless steel "sippers" permanently installed in each plot. Each sipper consisted of a length of stainless steel tubing, crimped and sealed at the end, with slits cut in the bottom 2 cm. The aboveground portion of each sipper was connected to Teflon tubing capped with a 2-way stopcock. Duplicate clusters of sippers were installed in each of the 30 plots at 20, 40, 80, and 120 cm below the soil surface. Porewater sitting in the sippers was drawn up and discarded, after which 60 mL of porewater from each depth (30 mL from each sipper) was withdrawn and stored in syringes equipped with 3-way stopcocks. Within 3 h, samples were filtered through preleached syringe filters (0.45 μm) and frozen until further analysis. NH_4 concentrations were measured using a Berthelot-salicylate colorimetric technique, modified to work in a 96-well microplate. Samples were run in triplicate and were all above the minimum detection limit of 0.05 ppm NH_4. Nitrate concentrations at this site are <0.05% of NH_4 concentrations (56), so NH_4 is assumed to represent all plant-available N. All depths were used for subsequent analysis.

Data Analysis. Data are plotted as means (n = 3) per treatment per year with SE indicated by error bars. Statistical analyses were conducted in R (version 3.4.3). We used linear mixed models with random intercepts to investigate the influence of warming and elevated CO_2 treatments on plant productivity and porewater chemistry. Warming was treated as a categorical variable [4 levels: Ambient, temp 1 (+1.7 °C), temp 2 (+3.4 °C), temp 3 (+5.1 °C)] to identify nonlinear effects, while year and transect (experimental block) were treated as random effects. We fit 3 separate models for each response variable: 1) C_3 warming-only plots (n = 12), 2) C_4 warming-only plots (n = 12), and 3) C_3 warming × eCO_2 plots (n = 12). Six C_3 plots (ambient temperature × ambient CO_2 and +5.1 °C × ambient CO_2) were included in both models 1 and 3. ANOVA tables and fixed effects results for each model are provided in *SI Appendix*. Tukey's post hoc tests were used to compare individual means. Pearson's correlations were used to investigate the relationship between porewater NH_4^+ and root biomass.

Data Availability. The data that support the findings of this study are included in *SI Appendix*.

1. C. Korner, Biosphere responses to CO_2 enrichment. *Ecol. Appl.* **10**, 1590–1619 (2000).
2. M. Lu *et al.*, Responses of ecosystem carbon cycle to experimental warming: A meta-analysis. *Ecology* **94**, 726–738 (2013).
3. W. C. Oechel *et al.*, Transient nature of CO_2 fertilization in Arctic tundra. *Nature* **371**, 500–503 (1994).
4. M. R. Shaw *et al.*, Grassland responses to global environmental changes suppressed by elevated CO_2. *Science* **298**, 1987–1990 (2002).
5. M. Fernández-Martínez *et al.*, Global trends in carbon sinks and their relationships with CO 2 and temperature. *Nat. Clim. Chang.* **9**, 73–79 (2019).
6. F. A. Dijkstra *et al.*, Contrasting effects of elevated CO_2 and warming on nitrogen cycling in a semiarid grassland. *New Phytol.* **187**, 426–437 (2010).
7. R. E. Sharwood, K. Y. Crous, S. M. Whitney, D. S. Ellsworth, O. Ghannoum, Linking photosynthesis and leaf N allocation under future elevated CO_2 and climate warming in *Eucalyptus globulus. J. Exp. Bot.* **68**, 1157–1167 (2017).
8. M. J. Hovenden *et al.*, Warming prevents the elevated CO_2-induced reduction in available soil nitrogen in a temperate, perennial grassland. *Glob. Change Biol.* **14**, 1018–1024 (2008).
9. O. Dermody, J. F. Weltzin, E. C. Engel, P. Allen, R. J. Norby, How do elevated [CO_2], warming, and reduced precipitation interact to affect soil moisture and LAI in an old field ecosystem? *Plant Soil* **301**, 255–266 (2007).
10. K. E. Mueller *et al.*, Impacts of warming and elevated CO_2 on a semi-arid grassland are non-additive, shift with precipitation, and reverse over time. *Ecol. Lett.* **19**, 956–966 (2016).
11. K. Yue *et al.*, Responses of nitrogen concentrations and pools to multiple environmental change drivers: A meta-analysis across terrestrial ecosystems. *Glob. Ecol. Biogeogr.* **28**, 690–724 (2019).
12. Y. Luo *et al.*, Progressive nitrogen limitation of ecosystem responses to rising atmospheric carbon dioxide. *Bioscience* **54**, 731–739 (2004).
13. J. A. Langley, J. P. Megonigal, Ecosystem response to elevated CO_2 levels limited by nitrogen-induced plant species shift. *Nature* **466**, 96–99 (2010).
14. P. B. Reich *et al.*, Nitrogen limitation constrains sustainability of ecosystem response to CO_2. *Nature* **440**, 922–925 (2006).
15. J. M. Craine *et al.*, Isotopic evidence for oligotrophication of terrestrial ecosystems. *Nat. Ecol. Evol.* **2**, 1735–1744 (2018).
16. D. P. Rasse, C. Rumpel, M.-F. Dignac, Is soil carbon mostly root carbon? Mechanisms for a specific stabilisation. *Plant Soil* **269**, 341–356 (2005).
17. M. C. Braakhekke *et al.*, Modeling the vertical soil organic matter profile using Bayesian parameter estimation. *Biogeosciences* **10**, 399–420 (2013).
18. T. Kätterer, M. A. Bolinder, O. Andrén, H. Kirchmann, L. Menichetti, Roots contribute more to refractory soil organic matter than above-ground crop residues, as revealed by a long-term field experiment. *Agric. Ecosyst. Environ.* **141**, 184–192 (2011).
19. N. W. Sokol, M. A. Bradford, Microbial formation of stable soil carbon is more efficient from belowground than aboveground input. *Nat. Geosci.* **12**, 46–53 (2019).
20. S. Xu, L. L. Liu, E. J. Sayer, Variability of above-ground litter inputs alters soil physicochemical and biological processes: A meta-analysis of litterfall-manipulation experiments. *Biogeosciences* **10**, 7423–7433 (2013).
21. G. Gyssels, J. Poesen, E. Bochet, Y. Li, Impact of plant roots on the resistance of soils to erosion by water: A review. *Prog. Phys. Geogr. Earth. Environ.* **29**, 189–217 (2005).
22. B. G. Drake, Rising sea level, temperature, and precipitation impact plant and ecosystem responses to elevated CO_2 on a Chesapeake Bay wetland: Review of a 28-year study. *Glob. Change Biol.* **20**, 3329–3343 (2014).
23. P. B. Reich, S. E. Hobbie, T. D. Lee, M. A. Pastore, Unexpected reversal of C_3 versus C_4 grass response to elevated CO_2 during a 20-year field experiment. *Science* **360**, 317–320 (2018).
24. X. Xu *et al.*, Interannual variability in responses of belowground net primary productivity (NPP) and NPP partitioning to long-term warming and clipping in a tallgrass prairie. *Glob. Change Biol.* **18**, 1648–1656 (2012).
25. J. S. Dukes *et al.*, Responses of grassland production to single and multiple global environmental changes. *PLoS Biol.* **3**, e319 (2005).
26. A. H. Baldwin, K. Jensen, M. Schönfeldt, Warming increases plant biomass and reduces diversity across continents, latitudes, and species migration scenarios in experimental wetland communities. *Glob. Change Biol.* **20**, 835–850 (2014).
27. A. J. Gray, R. J. Mogg, Climate impacts on pioneer saltmarsh plants. *Clim. Res.* **18**, 105–112 (2001).
28. H. Charles, J. S. Dukes, Effects of warming and altered precipitation on plant and nutrient dynamics of a New England salt marsh. *Ecol. Appl.* **19**, 1758–1773 (2009).
29. K. B. Gedan, M. D. Bertness, Experimental warming causes rapid loss of plant diversity in New England salt marshes. *Ecol. Lett.* **12**, 842–848 (2009).
30. K. B. Gedan, M. D. Bertness, How will warming affect the salt marsh foundation species *Spartina patens* and its ecological role? *Oecologia* **164**, 479–487 (2010).
31. K. B. Gedan, A. H. Altieri, M. D. Bertness, Uncertain future of New England salt marshes. *Mar. Ecol. Prog. Ser.* **434**, 229–238 (2011).
32. M. L. Kirwan, G. R. Guntenspergen, J. T. Morris, Latitudinal trends in *Spartina alterniflora* productivity and the response of coastal marshes to global change. *Glob. Change Biol.* **15**, 1982–1989 (2009).
33. K. Więski, S. C. Pennings, Climate drivers of *Spartina alterniflora* saltmarsh production in Georgia, USA. *Ecosystems* **17**, 473–484 (2014).
34. J. R. Giurgevich, E. L. Dunn, Seasonal patterns of CO_2 and water vapor exchange of the tall and short height forms of Spartina alterniflora Loisel in a Georgia salt marsh. *Oecologia* **43**, 139–156 (1979).
35. E. D. Seneca, U. Blum, Response to photoperiod and temperature by *Spartina alterniflora* (Poaceae) from North Carolina and *Spartina foliosa* from California. *Am. J. Bot.* **71**, 91–99 (1984).
36. R. F. Sage, D. S. Kubien, The temperature response of $C(_3)$ and $C(_4)$ photosynthesis. *Plant Cell Environ.* **30**, 1086–1106 (2007).
37. Y. Luo, S. Wan, D. Hui, L. L. Wallace, Acclimatization of soil respiration to warming in a tall grass prairie. *Nature* **413**, 622–625 (2001).
38. S. R. Saleska, J. Harte, M. S. Torn, The effect of experimental ecosystem warming on CO_2 fluxes in a montane meadow. *Glob. Change Biol.* **5**, 125–141 (1999).
39. C. Luo *et al.*, Effect of warming and grazing on litter mass loss and temperature sensitivity of litter and dung mass loss on the Tibetan plateau. *Glob. Change Biol.* **16**, 1606–1617 (2010).
40. J. M. Melillo *et al.*, Long-term pattern and magnitude of soil carbon feedback to the climate system in a warming world. *Science* **358**, 101–105 (2017).
41. J. A. Langley, K. L. McKee, D. R. Cahoon, J. A. Cherry, J. P. Megonigal, Elevated CO_2 stimulates marsh elevation gain, counterbalancing sea-level rise. *Proc. Natl. Acad. Sci. U.S.A.* **106**, 6182–6186 (2009).
42. F. S. Chapin, The mineral nutrition of wild plants. *Annu. Rev. Ecol. Syst.* **11**, 233–260 (1980).
43. H. Poorter *et al.*, Biomass allocation to leaves, stems and roots: Meta-analyses of interspecific variation and environmental control. *New Phytol.* **193**, 30–50 (2012).
44. S. M. Butler *et al.*, Soil warming alters nitrogen cycling in a New England forest: implications for ecosystem function and structure. *Oecologia* **168**, 819–828 (2012).
45. S. M. Schaeffer, E. Sharp, J. P. Schimel, J. M. Welker, Soil-plant N processes in a High Arctic ecosystem, NW Greenland are altered by long-term experimental warming and higher rainfall. *Glob. Change Biol.* **19**, 3529–3539 (2013).
46. L.-N. Ma *et al.*, The effects of warming and nitrogen addition on soil nitrogen cycling in a temperate grassland, northeastern China. *PLoS One* **6**, e27645 (2011).
47. G. M. Cott, J. S. Caplan, T. J. Mozdzer, Nitrogen uptake kinetics and saltmarsh plant responses to global change. *Sci. Rep.* **8**, 5393 (2018).
48. J. C. Carey, K. D. Kroeger, B. Zafari, J. Tang, Passive experimental warming decouples air and sediment temperatures in a salt marsh. *Limnol. Oceanogr. Methods* **16**, 640–648 (2018).
49. M. F. Arndal, A. Tolver, K. S. Larsen, C. Beier, I. K. Schmidt, Fine root growth and vertical distribution in response to elevated CO_2, warming and drought in a mixed heathland–grassland. *Ecosystems* **21**, 15–30 (2018).
50. IPCC Climate Change, "Synthesis report. Contribution of working groups I, II and III to the fifth assessment report of the intergovernmental panel on climate change" (IPCC, Geneva, Switzerland, 2014).
51. A. E. Raftery, A. Zimmer, D. M. W. Frierson, R. Startz, P. Liu, Less than 2 °C warming by 2100 unlikely. *Nat. Clim. Chang.* **7**, 637–641 (2017).
52. M. L. Kirwan, J. P. Megonigal, Tidal wetland stability in the face of human impacts and sea-level rise. *Nature* **504**, 53–60 (2013).
53. L. Cheng *et al.*, Recent increases in terrestrial carbon uptake at little cost to the water cycle. *Nat. Commun.* **8**, 110 (2017).
54. R. L. Rich *et al.*, Design and performance of combined infrared canopy and belowground warming in the B4WarmED (Boreal Forest Warming at an Ecotone in Danger) experiment. *Glob. Change Biol.* **21**, 2334–2348 (2015).
55. M. Lu *et al.*, Allometry data and equations for coastal marsh plants. *Ecology* **97**, 3554 (2016).
56. R. Matamala, B. G. Drake, The influence of atmospheric CO_2 enrichment on plant-soil nitrogen interactions in a wetland plant community on the Chesapeake Bay. *Plant Soil* **210**, 93–101 (1999).